*Inorg. Chem.* **2004**, *43*, 8162–8168


# Structural and Conformational Properties of Fluoroformic Acid Anhydride, FC(O)OC(O)F

**Florian Mayer,[†] Heinz Oberhammer,*[,†] Michael Berkei,[‡] Holger Pernice,[‡] Helge Willner,*[,‡] Karina Bierbrauer,[§] Maximiliano Burgos Paci,[§] and Gustavo A. Argüello[§]**

*Institut für Physikalische und Theoretische Chemie, Universität Tübingen, D-72076 Tübingen, Germany, and FB C, Anorganische Chemie, Universität Wuppertal, D-42119 Wuppertal, Germany, and INFIQC, Departamento de Fisico Quimica, Universidad Nacional de Córdoba, 5000 Córdoba, Argentina*

Received June 17, 2004

The conformational properties and geometric structures of fluoroformic acid anhydride, FC(O)OC(O)F, have been studied by vibrational spectroscopy, gas electron diffraction (GED), single-crystal X-ray diffraction, and quantum chemical calculations (HF, MP2, and B3LYP methods with 6-31G* and B3LYP/6-311+G* basis sets). Satellite bands in the IR matrix spectra, which increase in intensity when the matrix gas mixture is heated prior to deposition as a matrix, indicate the presence of two conformers at room temperature. According to the electron diffraction analysis, the prevailing conformer is of $C_2$ symmetry with both C═O bonds synperiplanar with respect to the opposite C–O bond ([sp, sp] conformer). The minor conformer [15(5)% from IR matrix and 6(11)% from GED] is predicted by quantum chemical calculations to possess an [sp, ac] structure. FC(O)OC(O)F crystallizes in the orthorhombic system in the space group $P2_12_12_1$ with $a = 6.527(1)$ Å, $b = 7.027(1)$ Å, and $c = 16.191(1)$ Å and four formula units per unit cell. In the crystal, only the [sp, sp] conformer is present, and the structural parameters are very similar to those determined by GED.

## Introduction

The first evidence for the existence of fluoroformic acid anhydride, FC(O)OC(O)F [which can alternatively be named bis(fluoroformyl)ether] came from gas-phase kinetic measurements in smog chambers. Bednarek et al. studied the FTIR spectra of the FC(O)C(O)F photolysis products in an oxygen atmosphere,[1] whereas Goto et al. analyzed the Cl-atom-initiated depletion products of $FCH_2OCH_2F$.[2] Recently, a synthesis of FC(O)OC(O)F on the preparative scale has been developed by a gas-phase reaction between FC(O)OOC(O)F and CO.[3] Subsequently, this missing link in the family of $FC(O)O_xC(O)F$ molecules ($x = 0$,[4] 1,[3] 2,[5] 3,[6]) has been characterized comprehensively.[3] FC(O)OC(O)F is a moisture-sensitive colorless liquid with a boiling point of 19 °C and a melting point of −46 °C. Above 50 °C, it slowly decomposes to give $COF_2$ and $CO_2$. The $^{19}F$ and $^{13}C$ NMR spectra are consistent with an ABX spin system, and the evaluated NMR data fit nicely among those of the series of compounds $FC(O)O_xC(O)F$, $x = 0-3$. The new anhydride was further characterized by gas density measurements, mass spectrometry, and gas-phase IR and UV spectroscopy.[3] In this contribution, we report the first structural study of FC(O)OC(O)F in the gas phase as well as in the solid state, together with a detailed vibrational analysis to elucidate its conformational properties. The experimental investigations are supported by quantum chemical calculations.

Structural and conformational properties of compounds with two adjacent carbonyl groups of the type XC(O)−M−C(O)X with X = H, F, $CF_3$, or $OCF_3$ and M = $CH_2$, $CF_2$, O, or S have attracted much interest from

* To whom correspondence should be addressed. E-mail: heinz.oberhammer@uni-tuebingen.de (H.O.), willner@uni-wuppertal.de (H.W.).
† Universität Tübingen.
‡ Universität Wuppertal.
§ Universidad Nacional de Córdoba.

(1) Bednarek, G.; Argüello, G. A.; Zellner, R. *Ber. Bunsen-Ges. Phys. Chem.* **1996**, *100*, 445.
(2) Goto, M.; Kawasaki, M.; Wallington, T. J.; Hurley, M. D.; Sharratt, A. P. *Int. J. Chem. Kinet.* **2002**, *34*, 139.
(3) Pernice, H.; Willner, H.; Bierbrauer, K.; Burgos Paci, M.; Argüello, G. A. *Angew. Chem., Int. Ed.* **2002**, *41*, 3832.
(4) Fukuhara, N.; Bigelow, L. A. *J. Am. Chem. Soc.* **1941**, *63*, 788.
(5) Arvia, A. J.; Aymonino, P. J.; Waldow, C. H.; Schumacher, H. J. *Angew. Chem.* **1960**, *72*, 169.
(6) Pernice, H.; Berkei, M.; Henkel, G.; Willner, H.; Argüello, G. A.; McKee, M. L.; Webb, T. R. *Angew. Chem., Int. Ed.* **2004**, *43*, 2843.



10.1021/ic049210t CCC: $27.50 
Published on Web 11/05/2004

**Chart 1**

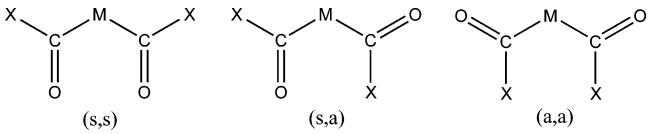


experimentalists and theoreticians. The orientation of each carbonyl group relative to the opposite M−C bond can be synperiplanar (sp), synclinal (sc), anticlinal (ac), or antiperiplanar (ap). The abbreviation sp corresponds to dihedral angles $\phi$(C−M−C═O) of 0 ± 30°, sc to 60 ± 30°, ac to 120 ± 30°, and ap to 180 ± 30°. The three possible conformations for such compounds are shown in Chart 1, where s can be sp or sc and a can be ap or ac. Malonyl difluoride, FC(O)−$CH_2$−C(O)F,[7] and malonyl dichloride, ClC(O)−$CH_2$−C(O)Cl,[8] for which only the diketo tautomer was observed, as well as difluoromalonyl difluoride, FC(O)−$CF_2$−C(O)F,[7] exist according to gas electron diffraction (GED) studies as mixtures of two conformers possessing either $C_1$ symmetry with [sp, ac] orientations or $C_2$ symmetry with [ac, ac] orientations. Whereas the $C_1$ conformer is favored in the two compounds with M = $CH_2$, the $C_2$ form prevails in difluoromalonyl difluoride. To our knowledge, the only compound with M = S whose structural properties have been determined is diacetyl sulfide, MeC(O)−S−C(O)Me.[9] For this compound, a single conformer with a planar heavy-atom skeleton, $C_s$ symmetry, and [sp,ap] orientations of the two C═O bonds has been observed. The conformational properties of anhydrides, XC(O)−O−C(O)X, depend on the substituents X. The parent compound, formic anhydride, HC(O)−O−C(O)H, has been studied extensively by GED,[10,11] microwave spectroscopy,[12] and quantum chemical calculations.[13] All investigations result in a planar [sp,ap] conformation that is stabilized by an intramolecular O···H bond. For acetic acid anhydride, MeC(O)−O−C(O)Me, two GED studies result in different conformational properties. Whereas the earlier investigation results in a single conformer with $C_2$ symmetry and [sc,sc] orientations of the two C═O bonds,[14] the more recent study results in a 2:1 mixture of [sp, ac] and [sp, sp] forms.[15] This latter result is confirmed by quantum chemical calculations. For perfluoroacetic acid anhydride, $CF_3$C(O)−O−C(O)$CF_3$, only a single conformer has been observed in a GED analysis with a slightly nonplanar skeleton of $C_2$ symmetry and an [sp, sp] orientation.[16,17]

## Experimental Section

*Caution: The starting material FC(O)OOC(O)F is potentially explosive if heated or brought into contact with oxidizable materials. It is thus recommended that appropriate safety precautions be taken when this compound is handled. Reactions involving FC(O)OOC(O)F should be carried out only in millimolar quantities.*

**General Procedures and Reagents.** Volatile materials were manipulated in a glass vacuum line equipped with two capacitance pressure gauges (221 AHS-1000 and 221 AHS-10, MKS Baratron, Burlington, MA), three U-traps, and valves with PTFE stems (Young, London, U.K.). The vacuum line was connected to the reactor and to an IR gas cell (optical path length 200 mm, Si wafers as windows) placed in the sample compartment of an FTIR instrument (Nicolet, Impact 400D). This allowed us to follow the course of the reaction and to observe the purification process. The starting materials FC(O)OOC(O)F,[18] FC(O)I,[19] and FC(O)$OCF_3$[20] were prepared according to literature procedures and stored in flame-sealed glass ampules under liquid nitrogen in a long-term Dewar vessel. The ampules were opened with an ampule key[21] on the vacuum line, appropriate amounts were removed for the experiments, and then the ampules were flame-sealed again.

The synthesis of FC(O)OC(O)F was performed in a clean, dry glass bulb of 1-L capacity previously conditioned for 1 h with 100 mbar of FC(O)OOC(O)F. After thorough pumping of the reaction vessel, 2 mmol of FC(O)OOC(O)F and 20 mmol of CO were introduced. The mixture was kept at 60 °C for several hours until most of the peroxide had disappeared. This was checked by IR spectroscopy of small samples taken from the reaction mixture. After cooling to −196 °C and removal of the unreacted CO in vacuo, the reaction mixture was separated by trap-to-trap condensation at −70, −120, and −196 °C. FC(O)OC(O)F was collected together with the unreacted peroxide in the trap at −120 °C. Fractions of several synthetic runs were collected and separated from the peroxide by evaporating the peroxide from the mixture at −95 °C until a pure sample of FC(O)OC(O)F remained in the trap. The yield of FC(O)OC(O)F related to the consumed peroxide was about 30%, and its purity according to IR and NMR spectra was about 98%. Attempted synthesis by reacting FC(O)I with HgO or FC(O)$OCF_3$ with $SO_3$/$H_2SO_4$ at room temperature failed. In the first case, only the decomposition products ($CO_2$ and $COF_2$) were observed, and in the second case, there was no reaction at all.

Matrix-isolated samples were prepared by passing a gas stream of argon or neon (~3 mmol $h^{-1}$) over a small sample (0.1 mmol) placed in a small U-trap in front of the matrix support and held at −110 °C. In this manner, the resulting sample-to-matrix gas ratio (estimated to be 1:1000) was immediately quenched on the matrix support (a rhodium-plated copper block with two mirror surfaces, made by courtesy of Umicore Company, Schwäbisch Gemünd, Germany) at 15 or 6 K. To influence the conformational mixture of FC(O)OC(O)F, the gas stream passed the spray-on nozzle at different temperatures prior to matrix deposition. Details of the matrix-isolation apparatus have been given elsewhere.[22]

(7) Jin, A.; Mack, H.-G.; Waterfeld, A.; Oberhammer, H. *J. Am. Chem. Soc.* **1991**, *113*, 7848.
(8) Mack, H.-G.; Oberhammer, H.; Della Vedova, C. O. *J. Mol. Struct.* **1995**, *346*, 51.
(9) Romano, R. M.; Della Vedova, C. O.; Downs, A. J.; Oberhammer, H.; Parson, S. *J. Am. Chem. Soc.* **2001**, *123*, 12623.
(10) Boogaard, A.; Geise, H. J.; Mijlhoff, F. C. *J. Mol. Struct.* **1972**, *13*, 53.
(11) Wu, G.; Shlykov, S.; Van Alsenoy, C.; Geise, H. J.; Sluyts, E.; Van der Veken, B. *J. Phys. Chem.* **1995**, *99*, 8589.
(12) Vaccani, S.; Roos, U.; Bauder, A.; Günthard, H. H. *Chem. Phys.* **1977**, *19*, 51.
(13) Lundell, J.; Rasanen, M.; Raaska, T.; Nieminen, J.; Murto, H. *J. Phys. Chem.* **1993**, *97*, 4577.
(14) Vledder, H. J.; Mijlhoff, F. C.; Leyte, J. C.; Romers, C. *J. Mol. Struct.* **1971**, *7*, 471.
(15) Wu, G.; Van Alsenoy, C.; Geise, H. J.; Sluyts, E.; Van der Veken, B.; Shishkov, I.; Khristenko, L. V. *J. Phys. Chem. A* **2000**, *104*, 1576.
(16) Andreassen, A. L.; Zebelman, D.; Bauer, S. H. *J. Am. Chem. Soc.* **1971**, *93*, 1148.
(17) Hermann, A.; Oberhammer, H. *J. Fluorine Chem.* **2004**, *125*, 917.
(18) Russo, A.; DesMarteau, D. D. *Inorg. Chem.* **1995**, *34*, 6221.
(19) Chiappero, M. S.; Argüello, G. A.; Garcia, P.; Pernice, H.; Willner, H.; Oberhammer, H.; Peterson, K. A.; Francisco, J. S. *Chem. Eur. J.* **2004**, *10*, 917.
(20) Hermann, A.; Trautner, F.; Gholivand, K.; v. Ahsen, S.; Varetti, E. L.; Della Vedova, C. O.; Willner, H.; Oberhammer, H. *Inorg. Chem.* **2001**, *40*, 3979.
(21) Gombler, W.; Willner, H. *J. Phys. E* **1987**, *20*, 1286.

For Raman measurements, a small sample spot was condensed on a cold copper finger at −196 °C under high vacuum in a homemade low-temperature cell.

**Instrumentation. (i) Vibrational Spectroscopy.** Infrared gas-phase and matrix spectra were recorded on an IFS-66v FT spectrometer (Bruker, Karlsruhe, Germany) with resolutions of 1 and 0.3 $cm^{-1}$, respectively. A DTGS detector, together with a Ge/KBr beam splitter, was operated in the region 4000−400 $cm^{-1}$, and 128 scans were typically collected for each spectrum. Raman spectra were recorded with a Bruker RFS 100/S FT Raman instrument in the region 3500−80 $cm^{-1}$ with a spectral resolution of 4 $cm^{-1}$, using the 1064-nm exciting line (∼500 mW) of a Nd:YAG laser.

**(ii) Single-Crystal X-ray Diffraction.** About 50 mg of FC(O)OC(O)F was placed in a flame-sealed and evacuated 6-mm glass tube. After storage of this glass ampule for several days on dry ice at −78 °C, small single crystals were formed. Then the ampule was opened in a cold stream of dry nitrogen at about −90 °C, and suitable crystals were transferred under a microscope into Lindemann capillaries as described in the literature.[23] X-ray diffraction data of a crystal at −130 °C were collected on a Nonius Kappa CCD diffractometer with graphite-monochromatized Mo Kα radiation. The data collection covered almost the whole sphere of reciprocal space with four sets at different $\kappa$ angles and 392 frames via $\omega$ rotation ($\Delta/\omega = 1°$) two times per frame for 40 s. No crystal decay was monitored by repeating the initial frames at the end of data collection. For technical reasons, it was not possible to perform an experimental absorption correction. Using the data reduction software SCALEPACK,[24] each measured frame is multiplied by a certain scale factor, which is generated by comparing the intensity of symmetrically related reflections.

For FC(O)OC(O)F, 3862 reflections were merged to 1381 independent reflections with $R$(int) = 0.0288. Thus data reduction with SCALEPACK worked, as is shown by the small $R$(int) value. The structure was solved by direct methods SHELXS97[24] and successive difference Fourier syntheses. Refinement applied full-matrix least-squares methods SHELXL97.[25] Atomic scattering factors for neutral atoms and real and imaginary dispersion terms were taken from the *International Tables for X-ray Crystallography*.[26] The figures were created by SHELXTL.[27] The crystal data are summarized in Table 1.

**(iii) Gas Electron Diffraction (GED).** Electron diffraction intensities were recorded with a Gasdiffractograph KD-G2[28] at 25- and 50-cm nozzle-to-plate distances and with an accelerating voltage of about 60 kV. The sample was cooled to −36 °C, and the inlet system and nozzle were at room temperature. The photographic plates were analyzed with the usual methods.[29] Average molecular intensities in the $s$ ranges 2−18 and 8−35 $Å^{-1}$ [$s = (4\pi/\lambda)\sin\vartheta/2$, where $\lambda$ is the electron wavelength and $\vartheta$ is the scattering angle] are shown in Figure 1.


(22) Schnöckel, H.; Willner, H. In *Infrared and Raman Spectroscopy, Methods and Applications*; Schrader, B., Ed.; VCH: Weinheim, Germany, 1994; p 297.
(23) Veith, M.; Bärnighausen, H. *Acta Crystallogr. B* **1974**, *30*, 1806.
(24) Sheldrick, G. M. *Acta Crystallogr. A* **1990**, *46*, 467.
(25) Sheldrick, G. M. *SHELXL97*; University of Göttingen: Göttingen, Germany, 1997.
(26) *International Tables for Crystallography*; Kluwer Academic Publishers: Dordrecht, The Netherlands, 1992; Vol. C.
(27) Sheldrick, G. M. *SHELXTL. Release 5.1 Software Reference Manual*; Bruker AXS, Inc.: Madison, WI, 1997.
(28) Oberhammer, H. *Molecular Structure by Diffraction Methods*; The Chemical Society: London, 1976; Vol. 4, p 24.
(29) Oberhammer, H.; Gombler, W.; Willner, H. *J. Mol. Struct.* **1981**, *70*, 273.


**Table 1.** Crystallographic Data for FC(O)OC(O)F

| | |
|---|---|
| empirical formula | $C_2F_2O_3$ |
| molar mass (g $mol^{-1}$) | 110.02 |
| space group | $P2_12_12_1$ |
| $a$ (Å) | 6.527(1) |
| $b$ (Å) | 7.027(1) |
| $c$ (Å) | 16.191(1) |
| $V$ ($Å^3$) | 742.6(2) |
| $D_{calc}$ (g $cm^{-3}$) | 1.968 |
| $Z$ | 4 |
| $\mu$ ($mm^{-1}$) | 0.241 |
| $T$ (°C) | −130(2) |
| $\lambda$ (Å) | 0.71069 |
| $R^a$ ($I > 2\sigma$) | R1 = 0.0227, wR2 = 0.0358 |
| $R^a$ (all data) | R1 = 0.0417, wR2 = 0.0374 |

[a] $R = \sum||F_o| - |F_c||/\sum|F_o|$. Refinement method: full-matrix least-squares calculations based on $F^2$.

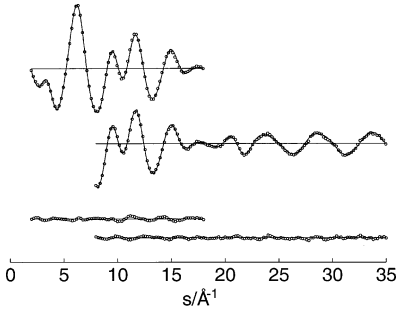


**Figure 1.** Experimental (points) and calculated (full line) molecular intensities for long (above) and short (below) nozzle-to-plate distances and residuals.

**Table 2.** Relative Energies $\Delta E$ and Gibbs Free Energies $\Delta G°$ in kJ/mol and Contribution in Percent of the Three Stable Conformers of FC(O)OC(O)F at 300 K

| | [sp, sp] | | | [sp, ac] | | | [ac, ac] | | |
|---|---|---|---|---|---|---|---|---|---|
| method | $\Delta E$ | $\Delta G°$ | contrib | $\Delta E$ | $\Delta G°$ | contrib | $\Delta E$ | $\Delta G°$ | contrib |
| HF/6-31G* | 0.0 | 0.0 | 92 | 5.1 | 6.1 | 8 | 14.6 | 15.0 | <1 |
| MP2/6-31G* | 0.0 | 0.0 | 98 | 7.1 | 9.7 | 2 | 13.4 | 15.3 | <1 |
| B3LYP/6-31G* | 0.0 | 0.0 | 91 | 4.7 | 6.1 | 8 | 10.6 | 11.5 | <1 |

## Quantum Chemical Calculations

A conformation of FC(O)OC(O)F is characterized by the torsional angles around the two O−C bonds, $\phi_1$(C2−O−C1=O) and $\phi_2$(C1−O−C2=O2). Geometry optimizations were performed with different starting values for $\phi_1$ and $\phi_2$, using the HF and MP2 approximations and the hybrid method B3LYP with 6-31G* basis sets. All three methods produce similar results and predict three stable conformers. Their relative energies and Gibbs free energies are listed in Table 2. The lowest-energy form exhibits a slightly nonplanar [sp, sp] structure with $C_2$ symmetry and $\phi_1 = \phi_2$ between 10 and 15°. An intermediate Gibbs free energy $\Delta G°$ between 4.7 and 7.1 kJ/mol is calculated for the [sp, ac] form with dihedral angles $\phi_1$ between 10° and 14° and $\phi_2$ between 131° and 145°. The [ac, ac] conformer with $C_2$ symmetry and $\phi_1 = \phi_2$ between 147° and 149° is predicted to have Gibbs free energies of 11.5−15.3 kJ/mol. The potential functions for the symmetric torsional motion, which have been derived for fixed values of $\phi_1 = \phi_2$ between 0° and 40°, are shown in Figure 2. All three methods predict double-minimum potentials with barriers at $\phi_1 = \phi_2 = 0°$ of 0.27 kJ/mol (HF), 0.05 kJ/mol (MP2), and 0.07 kJ/mol (B3LYP).

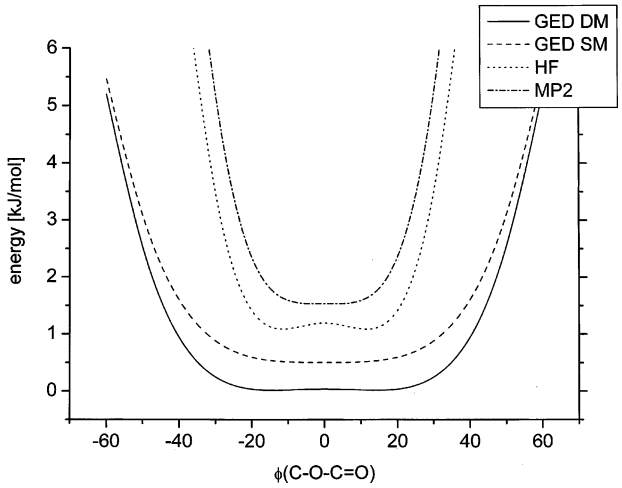


**Figure 2.** Calculated (MP2 and HF with 6-31G* basis sets) and experimental (GED) potential functions for symmetric torsion around the O−C bonds. GED DM curve corresponds to a double-minimum potential, GED SM to a single-minimum potential. The individual curves are shifted by 0.5 kJ/mol.

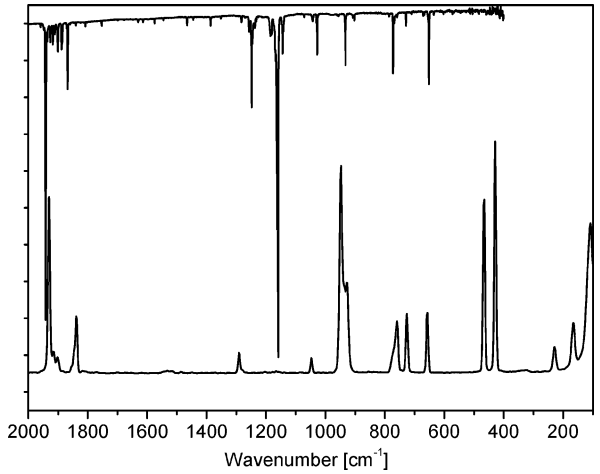


**Figure 3.** IR spectrum of FC(O)OC(O)F isolated in a Ne matrix (upper trace) and Raman spectrum of solid FC(O)OC(O)F at −196 °C (lower trace).

The functions derived with the MP2 and B3LYP methods are very similar, and only the former and that derived with the HF approximation are shown in Figure 2. All quantum chemical calculations were performed with the Gaussian 98 program package.[30] Vibrational frequencies of the [sp, sp] and [sp, ac] conformers were calculated with the B3LYP/6-311+G* method. Vibrational amplitudes were derived from these Cartesian force constants using the program ASYM40.[31]

## Vibrational Spectroscopy

The IR spectrum of FC(O)OC(O)F isolated in a Ne matrix and the Raman spectrum of solid FC(O)OC(O)F are both depicted in Figure 3.

All experimental vibrational data of the fundamentals are compared with calculated band positions and IR intensities in Table 3.

According to the quantum chemical calculations (see above), the global minimum structure of FC(O)OC(O)F exhibits a slightly nonplanar [sp, sp] structure with $C_2$ symmetry

**Table 3.** Observed and Calculated Vibrational Wavenumbers for the Fundamentals of [sp, sp] FC(O)OC(O)F

| IR | | | | | Raman | assignm acc | | appox descrip |
|---|---|---|---|---|---|---|---|---|
| gas phase | Ne matrix[a] | rel int[b] (%) | calcd[c] | rel int[c] (%) | solid[d] | $C_2$ symm | | of mode |
| 1941 | 1942.0 | 58 | 1987 | 55 | 1931(s) | A | $\nu_1$ | $\nu_s$(CO) |
| 1870 | 1868.0 | 8 | 1910 | 9 | 1838(m) | B | $\nu_9$ | $\nu_{as}$(CO) |
| 1249 | 1249.0 | 25 | 1229 | 6 | 1291(w) | A | $\nu_2$ | $\nu_s$(CF) |
| 1168 | 1159.2 | 100 | 1142 | 100[e] | − | B | $\nu_{10}$ | $\nu_{as}$(COC) |
| 1030 | 1027.9 | 5 | 1027 | 9 | 1048(w) | B | $\nu_{11}$ | $\nu_{as}$(CF) |
| 938 | 933.0 | 6 | 928 | 4 | 948(vs) | A | $\nu_3$ | $\nu_s$(COC) |
| 765 | 772.7 | 6 | 772 | 5 | 773(sh) | B | $\nu_{12}$ | $\delta$($FCO_2$)oop |
| − | − | − | 769 | 0.2 | 759(m) | A | $\nu_4$ | $\delta$($FCO_2$)oop |
| − | 729.2 | 1 | 711 | 0.5 | 726(m) | A | $\nu_5$ | $\delta_s$(O=CF) |
| 652 | 652.3 | 8 | 652 | 4 | 658(m) | B | $\nu_{13}$ | $\delta_{as}$(O=CF) |
| | | | 467 | <0.1 | 467(s) | B | $\nu_{14}$ | $\delta_{as}$(O−CF) |
| | | | 413 | <0.1 | 429(vs) | A | $\nu_6$ | $\delta_s$(O−CF) |
| | | | 204 | <0.1 | 230(w) | A | $\nu_7$ | $\delta$(COC) |
| | | | 122 | 0.1 | 166(m) | B | $\nu_{15}$ | $\tau_{as}$ |
| | | | 37 | <0.1 | | A | $\nu_8$ | $\tau_s$ |

[a] Most intensive matrix site. [b] Relative integrated intensity. [c] B3LYP functional with 6-311+G(d) basis set. [d] −196 °C. [e] Absolute intensity = 1222 km $mol^{-1}$.

and therefore the 15 fundamentals correspond to the irreducible representation

$$\Gamma_{vib} = 8A\ (IR, Raman) + 7B\ (IR, Raman)$$

The six stretching, seven bending, and two torsional modes are unambiguously assigned by their characteristic band positions, relative intensities in the IR and Raman spectra, and comparison with the calculated data (see Table 3). With the exception of the lowest torsional mode $\nu_8$, all fundamentals were observed. In general, the agreement between calculated and observed band positions is excellent, with the exception of the two $\nu$(CO) band positions, which are overestimated by about 50 $cm^{-1}$. The deviations between calculated and observed band positions in the Raman spectrum are due to interactions of the molecules in the solid state. Some absorptions in the IR matrix spectra are accompanied by satellites with 10−20% of the intensity of the main bands. Four small satellites can be seen between the two $\nu$(CO) bands of the main [sp, sp] rotamer. They are due to the two $\nu$(CO) bands of the less stable rotamer disturbed by Fermi resonances. The band positions of both Fermi couples were averaged, resulting in 1910 and 1895 $cm^{-1}$ as the position of the corrected $\nu$(CO) fundamentals. Further satellites are located at 1161, 759, and 665 $cm^{-1}$ (Ne matrix). Determination of all satellite intensities by integration is disturbed by overlapping bands due to matrix sites and

(30) Frisch, M. J.; Trucks, G. W.; Schlegel, H. B.; Scuseria, G. E.; Robb, M. A.; Cheeseman, J. R.; Zakrzewski, V. G.; Montgomery, J. A.; Stratman, R. E.; Burant, J. C.; Dapprich, S.; Millam, J. M.; Daniels, A. D.; Kudin, K. N.; Strain, M. C.; Farkas, O.; Tomasi, J.; Barone, V.; Cossi, M.; Cammi, R.; Menucci, B.; Pomelli, C.; Adamo, C.; Clifford, S.; Ochterski, J.; Petersson, G. A.; Ayala, P. Y.; Cui, Q.; Morokuma, K.; Malick, D. K.; Rabuck, A. D.; Raghavachari, K.; Foresman, J. B.; Cioslovski, J.; Ortiz, J. V.; Stefanov, B. B.; Liu, G.; Liashenko, A.; Piskorz, P.; Komaromi, I.; Gomperts, R.; Martin, R. L.; Fox, D. J.; Keith, T.; Al-Laham, M. A.; Peng, C. Y.; Nanayakkara, A.; Gonzales, C.; Challacombe, M.; Gill, P. M. W.; Johnson, B.; Chen, W.; Wong, M. W.; Andres, J. L.; Gonzales, C.; Head-Gordon, M.; Replogle; Pople, J. A. *Gaussian 98*, revision A.6; Gaussian Inc.: Pittsburgh, PA, 1998.
(31) Hedberg, L.; Mills, I. M. *J. Mol. Spectrosc.* **1993**, *160*, 117.

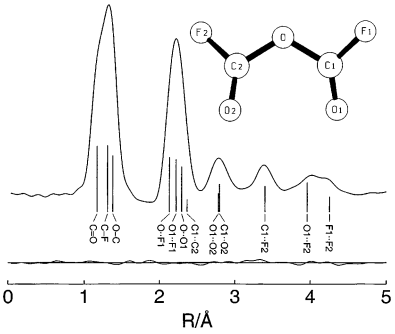


**Figure 4.** Experimental radial distribution function and difference curve. The interatomic distances corresponding to a rigid model are indicated by vertical bars.

**Table 4.** Interatomic Distances, Experimental and Calculated Vibrational Amplitudes in Å for FC(O)OC(O)F

| atom pair | dist | amplitude GED[a] | | B3LYP[b] | atom pair | dist | amplitude GED[a] | | B3LYP[b] |
|---|---|---|---|---|---|---|---|---|---|
| C=O | 1.17 | 0.034(4) | $l_1$ | 0.036 | C1···C2 | 2.37 | 0.065[c] | | 0.065 |
| C−F | 1.31 | 0.040(5) | $l_2$ | 0.043 | O1···O2 | 2.79 | 0.156[c] | | 0.156 |
| O−C | 1.38 | 0.043(5) | $l_2$ | 0.046 | C1···O2 | 2.79 | 0.094(11) | $l_4$ | 0.089 |
| O···F1 | 2.13 | 0.054(3) | $l_3$ | 0.056 | C1···F2 | 3.40 | 0.092(14) | $l_5$ | 0.076 |
| O1···F1 | 2.22 | 0.050[c] | | 0.050 | O1···F2 | 3.96 | 0.153(21) | $l_6$ | 0.174 |
| O···O1 | 2.29 | 0.052(2) | $l_3$ | 0.054 | F1···F2 | 4.25 | 0.095[c] | | 0.095 |

[a] Error limits are $3\sigma$ values. For atom numbering, see Figure 4. [b] 6-31G* basis sets. [c] Not refined.

impurities ($COF_2$). Therefore, only an estimate of the intensity can be given. The satellites grow in intensity by a factor of about 2 as the temperature of the deposition nozzle is increased from 300 to 560 K. It is most likely that these bands belong to the next most stable [sp, ac] form, with a contribution of about 15(5)% in the rotamer mixture at room temperature. This assumption is supported by comparing experimental and calculated (in parentheses) wavenumber differences between the band positions of the two conformers: 1942−1910 = 32 (28), 1942−1895 = 47 (51), 1159−1161 = −2 (−1), 773−759 = 14 (11), 652−665 = −3 (−3). The calculated wavenumbers and IR intensities for the fundamentals of the [sp, ac] rotamer are given in Table S1 in the Supporting Information. Furthermore, in the low-temperature Raman spectrum, obtained by quenching the room-temperature gas phase as a solid at −196 °C, shoulders can be seen on the bands at 1931, 948, and 773 $cm^{-1}$ that are due to the second rotamer (see Figure 3). The shoulder at 773 $cm^{-1}$ should also contain a contribution of the fundamental $\nu_{12}$ of the main rotamer (see Table 3).

## Electron Diffraction Analysis

The experimental radial distribution function (RDF), which was derived by Fourier transformation of the molecular intensities with an artificial damping function $\exp(-\gamma s^2)$, $\gamma = 0.0019$ Å$^2$, is shown in Figure 4. The RDF is reproduced best with a nonplanar [sp, sp] conformer. In the first step, a rigid structural model undergoing only small-amplitude vibrations was refined by least-squares fitting of the molecular intensities. In this refinement, the molecule was constrained to $C_2$ symmetry. Vibrational amplitudes were collected in groups (see Table 4), and amplitudes that either caused high correlations between geometric parameters or were poorly determined by the GED experiment were set to calculated values. With these assumptions, seven geometric parameters ($p_1-p_7$) and six vibrational amplitudes ($l_1-l_6$) were refined simultaneously. The following correlation coefficients had absolute values larger than 0.6: $p_1/p_2 = -0.61$, $p_3/p_5 = 0.64$, $p_1/l_2 = -0.80$, and $l_1/l_2 = 0.73$. The agreement factor was $R = 5.75\%$ [$R = \sum(s_i M_i^{exp} - M_i^{calc})^2/\sum(s_i M_i^{exp})^2$]. The results of this refinement are given in Table 4 (vibrational amplitudes) and Table 5 (geometric parameters), together with calculated values. The experimental dihedral angle $\phi$ obtained in this GED analysis represents an "effective" value because of a large-amplitude torsional vibration.

**Table 5.** Experimental and Calculated Geometric Parameters for FC(O)OC(O)F

| | GED[a] | | X-ray[b] | MP2[c] | B3LYP[c] | HF[c] |
|---|---|---|---|---|---|---|
| C=O | 1.172(2) | $p_1$ | 1.162(2) | 1.190 | 1.182 | 1.158 |
| O−C | 1.378(4) | $p_2$ | 1.362(2) | 1.376 | 1.371 | 1.342 |
| C−F | 1.309(3) | $p_3$ | 1.312(2) | 1.333 | 1.326 | 1.293 |
| C−O−C | 118.2(7) | $p_4$ | 117.8(2) | 118.2 | 119.6 | 121.5 |
| O−C=O | 128.0(4) | $p_5$ | 130.2(2) | 129.8 | 129.4 | 128.7 |
| O−C−F | 105.0(2) | $p_6$ | 104.9(2) | 104.7 | 105.2 | 106.2 |
| $\phi$(C−O−C=O) | 20.8(21) | $p_7$ | 10.0(3) | 9.6 | 12.0 | 15.4 |

[a] $r_a$ values in Å and deg, derived with a rigid molecular model. Error limits are $3\sigma$ values. For atom numbering, see Figure 4. [b] Mean values of the two crystallographically independent molecules in the unit cell. [c] 6-31G* basis sets.

In the next step, refinements were performed for mixtures of [sp, sp] and [sp, ac] conformers. According to all quantum chemical calculations, only these two forms are expected to be present in the gas phase, given that the third most stable structure has a free enthalpy greater than 11.5 kJ/mol. Bond lengths and angles of the [sp, ac] form were approximated to those of the main conformer with the calculated (MP2) differences. Dihedral angles $\phi_1$ and $\phi_2$ and all vibrational amplitudes were set to calculated values. The agreement factor decreased very slightly to $R = 5.73\%$ for a contribution of 6(11)% of the [sp, ac] conformer. Thus, GED data do not definitively establish the presence of a second conformer.

It is evident from the calculated torsional potential functions that a rigid model is not quite adequate for this molecule. The predicted frequencies for the symmetric torsional vibration are 31 (HF), 14 (MP2), and 20 $cm^{-1}$ (B3LYP). Therefore, the molecular intensities were fitted with a dynamic model that is composed of pseudo-conformers with $C_2$ symmetry and different dihedral angles $\phi$ from 0° to 60°. Each conformer is weighted by a Boltzmann factor. As suggested by the quantum chemical calculations, a double-minimum potential of the form $V = V_0[1 - (\phi/\phi_e)^2]^2$ was used. $V_0$ is the barrier at $\phi = 0°$, and $\phi_e$ is the equilibrium value for the dihedral angle corresponding to the minimum of the potential function. Vibrational amplitudes for torsion-dependent interatomic distances were set to values that were derived from the calculated force field without contributions from the torsional frequencies. Because of a high correlation between $V_0$ and $\phi_e$, it was not possible to refine both parameters simultaneously. Thus, refinements of bond lengths, bond angles, and $\phi_e$ with fixed $V_0$ values were performed. For $V_0 = 0.27$ kJ/mol (value predicted by the HF method),

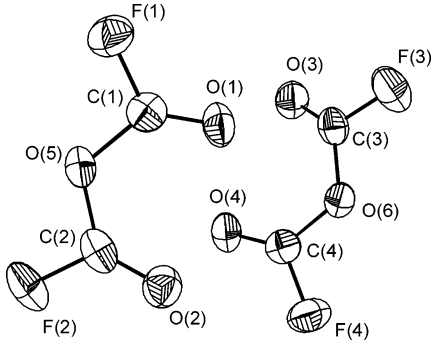


**Figure 5.** Projection of the two crystallographically independent FC(O)-OC(O)F molecules with their atom labeling. Thermal ellipsoids are drawn at the 50% probability level.

the refined dihedral angle was $\phi_e = 24.5(16)°$. The fit of the intensities was slightly better ($R = 5.52\%$) than that with the rigid model (5.75%). The fit of the intensities improved further for smaller values of $V_0$, and the agreement factor remained nearly constant (5.32−5.22%) for $V_0 \leq 0.10$ kJ/mol. The $\phi_e$ values decreased from 20.4(14) ° for $V_0 = 0.10$ kJ/mol to 15.3(14) ° for $V_0 = 0.01$ kJ/mol. All potential functions for the various ($V_0$, $\phi_e$) pairs, however, exhibit a very similar overall shape. The double-minimum potential with $V_0 = 0.05$ kJ/mol (value predicted by the MP2 method) and $\phi_e = 17.4(15)°$ is shown in Figure 2 (curve GED DM). In the final step of the GED analysis, a single-minimum quartic potential function, $V = k\phi^4$, was used for the torsional motion. In this refinement, the lowest agreement factor of $R = 5.12\%$ was obtained for $k = 4.2(12)$ kJ rad$^{-4}$. This potential function (see Figure 5, curve GED SM) is again very similar to the curves obtained with double-minimum potentials. The bond lengths and bond angles obtained with the various dynamic models agree with those of the rigid model (Table 5) within their error limits.

### X-ray Structure Determination

FC(O)OC(O)F crystallizes in the orthorhombic system in the space group $P2_12_12_1$ with $a = 6.527(1)$ Å, $b = 7.027(1)$ Å, and $c = 16.191(1)$ Å and four formula units per unit cell. Both crystallographically independent molecules are depicted in Figure 5. They exhibit an [sp, sp] structure as found in the GED experiments and as predicted from quantum chemical calculations. The chiral molecules with $C_2$ symmetry form a racemic mixture. All bond parameters are collected in Table 6.[32]

In addition, the Supporting Information contains more information about the crystal data and structure refinements (Table S2), atomic coordinates and equivalent isotropic displacement parameters (Table S3), and anisotropic displacement parameters (Table S4). The mean values of the geometric parameters are compared with the calculated and GED results in Table 5. In comparison with the GED results, there is general agreement between the geometric parameters, with the exception of the torsional angle. This is not surprising because even weak forces can change this inner coordinate.

(32) Klyne, W.; Prelog, V. *Experientia* **1960**, *16*, 521.

**Table 6.** Bond Lengths (Å), Angles (deg), and Torsion Angles for FC(O)O(O)CF (deg) in the Solid State

| | | | |
|---|---|---|---|
| **Bonds** | | | |
| C(1)−F(1) | 1.311(2) | C(2)−O(2) | 1.162(2) |
| C(2)−F(2) | 1.317(2) | C(2)−O(5) | 1.362(2) |
| C(3)−F(3) | 1.310(2) | C(3)−O(3) | 1.165(2) |
| C(4)−F(4) | 1.309(2) | C(3)−O(6) | 1.358(2) |
| C(1)−O(1) | 1.161(2) | C(4)−O(4) | 1.161(2) |
| C(1)−O(5) | 1.365(2) | C(4)−O(6) | 1.365(2) |
| **Angles**[a] | | | |
| F(1)−C(1)−O(1) | 125.1(2) | F(4)−C(4)−O(6) | 104.8(2) |
| F(1)−C(1)−O(5) | 104.72(13) | C(1)−O(5)−C(2) | 117.32(13) |
| F(2)−C(2)−O(2) | 124.9(2) | C(3)−O(6)−C(4) | 117.97(14) |
| F(2)−C(2)−O(5) | 104.8(2) | O(1)−C(1)−O(5) | 130.1(2) |
| F(3)−C(3)−O(3) | 124.6(2) | O(2)−C(2)−O(5) | 130.4(2) |
| F(3)−C(3)−O(6) | 105.2(2) | O(3)−C(3)−O(6) | 130.1(2) |
| F(4)−C(4)−O(4) | 125.1(2) | O(4)−C(4)−O(6) | 130.0(2) |
| **Torsion Angles**[a] | | | |
| C(1)−O(5)−C(2)−F(2) | −174.86(12) | C(3)−O(6)−C(4)−F(4) | 168.57(12) |
| C(1)−O(5)−C(2)−O(2) | 6.03(26) | C(3)−O(6)−C(4)−O(4) | −12.82(26) |
| C(2)−O(5)−C(1)−F(1) | −169.48(12) | C(4)−O(6)−C(3)−F(3) | 172.77(12) |
| C(2)−O(5)−C(1)−O(1) | 11.36(25) | C(4)−O(6)−C(3)−O(3) | −9.74(26) |

[a] Torsion/dihedral angles follow right-hand rule, Klyne and Prelog convention.[32]

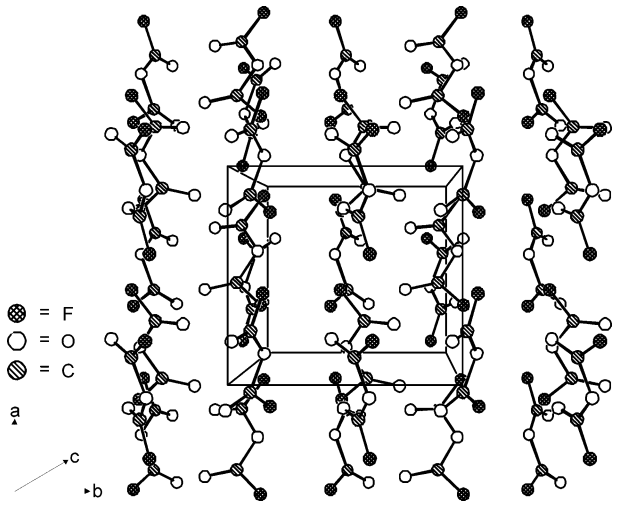


**Figure 6.** View of a part of the crystal structure of FC(O)OC(O)F in the *z* orientation with the unit cell. Thermal ellipsoids are drawn at the 50% probability level.

There are no obvious intermolecular interactions below the sum of the van der Waals radii of the corresponding atoms, as can be seen from Figure 6. Thus, the potentially important influence of packing effects on geometric parameters other than the torsional angle can be neglected.

### Discussion

According to IR(matrix) spectra and GED, FC(O)OC(O)F exists in the gas phase as a mixture of two conformers. The prevailing [sp, sp] form exhibits $C_2$ symmetry with both C═O bonds oriented synperiplanar. The minor conformer [15(5)% from IR(matrix) and 6(11)% from GED, corresponding to $\Delta G° = 4.3(9)$ and 6.8(47) kJ/mol, respectively] exhibits $C_1$ symmetry with synperiplanar and anticlinal orientation of the C═O bonds. The calculated $\Delta G°$ values (see Table 2) are slightly higher than the experimental value derived from the IR(matrix) spectra. For the [sp, sp] form, quantum chemical calculations predict a slightly nonplanar

structure with $C_2$ symmetry, torsional angles around the O−C bonds between 10° and 15°, and very low barriers for the planar structure of 0.05−0.27 kJ/mol. The GED intensities cannot distinguish between a single-minimum potential for the torsional motion, which corresponds to a planar equilibrium structure with very large-amplitude torsional vibration, and a double-minimum potential with a low barrier ($V_0$ < 0.10 kJ/mol), which corresponds to a pseudo-planar equilibrium structure with the barrier well below the zero-point vibrational energy. Independent of the detailed shape of the potential function, however, the experimental potential function (GED DM or GED SM in Figure 2) for the free molecule is considerably wider than the calculated functions. This implies a larger torsional equilibrium angle $\phi_e$ in the case of a double-minimum potential between 15° and 20° or a larger amplitude of the torsional vibration in the case of a single-minimum potential. Both cases are described with an "effective" torsional angle of 20.8(21)°. In the crystal, only the [sp, sp] conformer exists, and the weak intermolecular interactions due to packing lead to a smaller mean value for the dihedral angles of 10.0(3)°. In the isoelectronic $N_2O_5$ molecule, the two $NO_2$ groups also undergo large-amplitude torsional motions about a point of minimum energy corresponding to $C_2$ symmetry for the molecule with dihedral angles of about ±30°.[33] However, molecular $N_2O_5$ dissociates in the solid state into the ionic compound $NO_2^+NO_3^-$.[34] There is a parallel with the thermal decomposition of FC(O)OC(O)F into $CO_2$ and $COF_2$.

The torsional potential function is a delicate balance between steric repulsion between the two C═O bonds, which favors a nonplanar structure, and orbital interactions, which favor a planar structure. These orbital interactions are composed of conjugation between the p-shaped oxygen lone pair $n_\pi$(O) and the C═O $\pi^*$ bonds and of anomeric effects between the $sp^2$-shaped oxygen lone pair and the C═O and C−F $\sigma^*$ bonds. According to a natural bond orbital (NBO) analysis of the B3LYP wave function, the sum of these orbital interactions amounts to 434 kJ/mol for a perfectly planar structure. The stabilization energy decreases to 416 kJ/mol at $\phi = 12.0°$, which corresponds to the calculated minimum of the total energy. For the experimental structure with $\phi \approx 20°$, the orbital interaction energy decreases to 394 kJ/mol, i.e., 40 kJ lower than that for the exactly planar structure. Because the total energy changes very little between $\phi = 0°$ and $\phi = 20°$, we conclude that this loss in stabilization energy corresponds to the decrease in steric repulsion. The O···O contact increases from 2.66 Å for the planar structure to 2.79 Å for the experimental structure. The latter nonbonded distance corresponds closely to the van der Waals distance of 2.80 Å.

The conformational properties of FC(O)OC(O)F can also be rationalized qualitatively on the basis of orbital interactions. The [ac, ac] conformer, which is expected to be the sterically most favored structure, exhibits the highest relative total energy $\Delta E$, between 10.6 and 14.6 kJ/mol. On the other hand, its stabilization energy due to conjugation and anomeric interactions (256 kJ/mol) is much lower than that of the sterically unfavorable [sp, sp] form (416 kJ/mol for the calculated geometry). The [sp, ac] conformer, which is expected to experience an intermediate steric strain, also exhibits an intermediate total energy $\Delta E$ between 4.7 and 7.1 kJ/mol and an intermediate stabilization energy of 330 kJ/mol.

**Acknowledgment.** This work was supported by the Deutsche Forschungsgemeinschaft and Volkswagenstiftung. Professor Minkwitz (University of Dortmund) is gratefully acknowledged for allowing the use of the X-ray diffractometer. H.P., K.L.B., and M.B.P. acknowledge the receipt of travel expenses within the ANPCyT-DAAD Proalar program. M.B.P. thanks CONICET-Argentina for his postdoctoral fellowship.

**Supporting Information Available:** Table S1 of calculated vibrational wavenumbers and IR intensities for the [sp, ac] conformer of FC(O)OC(O)F, Table S2 of atomic coordinates and equivalent isotropic displacement parameters, Table S3 of bond lengths and angles, and Table S4 of anisotropic displacement parameters. This material is available free of charge via the Internet at http://pubs.acs.org. In addition, complete structure reports are available from Fachinformationzentrum Karlsruhe, D-76344 Eggenstein-Leopoldshaven, Hermann von Helmholtz Platz 1, Germany; e-mail, crystdata@Fiz.Karlsruhe.de; fax int, 49-7247-806-666. Deposit number CSD 414408 FC(O)OC(O)F.

IC049210T

(33) McClelland, B. W.; Hedberg, L.; Hedberg, K.; Hagen, K. *J. Am. Chem. Soc.* **1983**, *105*, 3789.
(34) Wilson, W. W.; Christe, K. O. *Inorg. Chem.* **1987**, *26*, 1631.